$\pi^0 \to \gamma^*\gamma$ transition form factor within the light-front quark model

Chong-Chung Lih[1,2,*] and Chao-Qiang Geng[2,3,†]
[1]*Department of Optometry, Shu-Zen College of Medicine and Management, Kaohsiung Hsien, Taiwan 452*
[2]*Physics Division, National Center for Theoretical Sciences, Hsinchu, Taiwan 300*
[3]*Department of Physics, National Tsing Hua University, Hsinchu, Taiwan 300*
(Received 8 December 2011; published 26 January 2012)

The transition form factor of $\pi^0 \to \gamma^*\gamma$ is studied as a function of the momentum transfer Q^2 within the light-front quark model (LFQM). Results are compared with the experimental data by the BABAR collaboration as well as other calculations based on the LFQM in the literature. It is shown that the predicted form factor fits well with the experimental data, particularly those at the large Q^2 region.

DOI: 10.1103/PhysRevC.85.018201 PACS number(s): 13.25.Cq, 13.40.Gp, 12.39.Ki, 24.85.+p

Introduction. The BABAR collaboration [1] has reported data of the $\pi^0 \to \gamma^*\gamma$ transition form factor $F_{\pi\gamma}(Q^2)$ for the high-momentum transfer Q^2 up to 40 GeV^2. To describe the data with the Q^2 dependence, the form factor is fitted to satisfy the formula

$$Q^2|F_{\pi\gamma}(Q^2)| = A\left(\frac{Q^2}{10\,\text{GeV}^2}\right)^{\beta} \quad (1)$$

with $A = 0.182 \pm 0.002$ GeV and $\beta = 0.25 \pm 0.02$. Before this data, most theoretical models predicted that the form factor approaches the QCD asymptotic limit [2], depending on the pion distribution amplitude (DA) with the Q^2 dependence under 10 GeV^2 [3–5]. Obviously, the experimental values for $Q^2 > 10$ GeV^2 by BABAR are surprisingly much higher than the QCD asymptotic expectations and thus, cannot be explained by the lowest perturbative results [2]. Even when the high-order corrections are considered [6,7], the large Q^2 behavior is still hard to be understood. Recently, many proposals [8–31] have been given in the literature to understand the transition form factor, particularly the BABAR data for $Q^2 > 10$ GeV^2.

In this Brief Note, we will use the phenomenological light-front (LF) pion wave function to evaluate $Q^2|F_{\pi\gamma}(Q^2)|$ in the light-front quark model (LFQM) [32–36]. We will concentrate on the spacelike region for the transition form factor. The LF wave function is manifestly boost invariant as it is expressed in terms of the longitudinal momentum fraction and relative transverse momentum variables. The parameter in the hadronic wave function is determined from other information and the meson state of the definite spins can be constructed by the Melosh transformation. We emphasize that our derivation of the form factor can be applied to all allowed kinematic regions. In Ref. [37], the study on the transition pion form factor based on the LFQM has been done but the calculation for Q^2 is only up to 8 GeV^2. With the same set of parameters in Ref. [37], the high-Q^2 BABAR data cannot be fitted. The use of the LFQM to understand the BABAR data has been explored in Ref. [38]. However, the conclusion in Ref. [38] has not explained the data. In this work, we would like to revisit the LFQM to see if this is indeed the case.

The form factor. The transition form factor of $F_{\pi^0\to\gamma^*\gamma^*}(q_1^2, q_2^2)$, which describes the vertex of $\pi^0\gamma^*\gamma^*$, is defined by

$$\begin{aligned} A[\pi^0(P) &\to \gamma^*(q_1,\epsilon_1)\gamma^*(q_2,\epsilon_2)] \\ &= ie^2 F_{\pi^0\to\gamma^*\gamma^*}(q_1^2,q_2^2)\varepsilon_{\mu\nu\rho\sigma}\epsilon_1^{\mu}\epsilon_2^{\nu}q_1^{\rho}q_2^{\sigma}\,, \end{aligned} \quad (2)$$

where $F_{\pi^0\to\gamma^*\gamma^*}(q_1^2, q_2^2)$ is a symmetric function under the interchange of q_1^2 and q_2^2. From the quark-meson diagram depicted in Fig. 1, the amplitude in Eq. (2) is found to be

$$\begin{aligned} &A[Q\bar{Q} \to \gamma^*(q_1)\gamma^*(q_2)] \\ &= e_Q e_{\bar{Q}} N_c \int \frac{d^4p_3}{(2\pi)^4}\Lambda_P \left\{ \mathrm{Tr}\left[\gamma_5 \frac{i(-\not{p}_3 + m_{\bar{Q}})}{p_3^2 - m_{\bar{Q}}^2 + i\epsilon} \right.\right. \\ &\quad \left.\times\ \not{\epsilon}_2 \frac{i(\not{p}_2 + m_Q)}{p_2^2 - m_Q^2 + i\epsilon}\ \not{\epsilon}_1 \frac{i(\not{p}_1 + m_Q)}{p_1^2 - m_Q^2 + i\epsilon}\right] \\ &\quad \left. + (\epsilon_1 \leftrightarrow \epsilon_2\,,\ q_1 \leftrightarrow q_2) \right\} \\ &\quad + (p_{1(3)} \leftrightarrow p_{3(1)}\,,\ m_Q \leftrightarrow m_{\bar{Q}})\,, \end{aligned} \quad (3)$$

where N_c is the number of colors, e_Q is the quark electric charge, and Λ_P is the vertex function related to the π^0 meson bound state. To calculate the $\pi^0 \to \gamma^*\gamma^*$ transition form factor within the LFQM, we have to decompose the π^0 meson into $Q\bar{Q}$ Fock states, described as $(u\bar{u} - d\bar{d})/\sqrt{2}$. In the LF approach, the LF meson wave function can be expressed by an antiquark $\bar{Q}$ and a quark Q with the total momentum P as

$$\begin{aligned} |M(P,S,S_z)\rangle = \sum_{\lambda_1\lambda_2}\int [dp_1][dp_2]2(2\pi)^3\delta^3(P - p_1 - p_2) \\ \times \Phi_M^{SS_z}(z,k_\perp)b_{\bar{Q}}^{+}(p_1,\lambda_1)d_Q^{+}(p_2,\lambda_2)|0\rangle\,, \end{aligned} \quad (4)$$

where

$$[dp] = \frac{dp^+d^2p_\perp}{2(2\pi)^3}\,, \quad (5)$$

*cclih@phys.nthu.edu.tw
†geng@phys.nthu.edu.tw

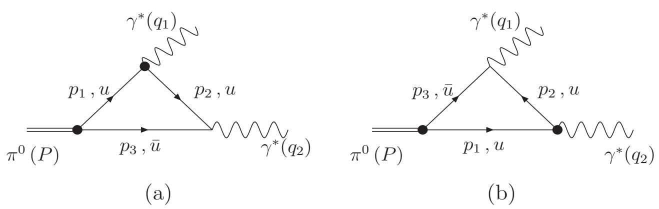

FIG. 1. Loop diagrams that contribute to $\pi^0 \to \gamma^*\gamma^*$.

$\Phi_M^{\lambda_1\lambda_2}$ is the amplitude of the corresponding $\bar{q}(q)$, and $p_{1(2)}$ is the on-mass shell LF momentum of the internal quark. In the momentum space, the wave function $\Phi_M^{SS_z}$ is given by

$$\Phi_M^{SS_z}(k_1, k_2, \lambda_1, \lambda_2) = R_{\lambda_1\lambda_2}^{SS_z}(z, k_\perp)\phi(z, k_\perp), \qquad (6)$$

where $\phi(z, k_\perp)$ represents the momentum distribution amplitude of the constituents in the bound state and $R_{\lambda_1\lambda_2}^{SS_z}$ constructs a spin state (S, S_z) out of light-front helicity eigenstates $(\lambda_1\lambda_2)$ [39]. The LF relative momentum variables $(z, k_\perp)$ are defined by

$$\begin{aligned} p_1^+ &= zP^+, \quad p_2^+ = (1-z)P^+ , \\ p_{1\perp} &= zP_\perp - k_\perp, \quad p_{2\perp} = (1-z)P_\perp + k_\perp . \end{aligned} \qquad (7)$$

The normalization condition of the meson state is given by

$$\begin{aligned} &\langle M(P', S', S_z')|M(P, S, S_z)\rangle \\ &\quad = 2(2\pi)^3 P^+ \delta^3(P' - P)\delta_{S'S}\delta_{S_z'S_z} , \end{aligned} \qquad (8)$$

which leads the momentum distribution amplitude $\phi(z, k_\perp)$ to

$$N_c \int \frac{dz\, d^2k_\perp}{2(2\pi)^3} |\phi(z, k_\perp)|^2 = 1 . \qquad (9)$$

We note that Eq. (6) can, in fact, be expressed as a covariant form [32,33,40]

$$\begin{aligned} \Phi_M^{SS_z}(z, k_\perp) &= \left(\frac{p_1^+ p_2^+}{2[M_0^2 - (m_Q - m_{\bar{Q}})^2]} \right)^{\frac{1}{2}} \\ &\quad \times \bar{u}(p_1, \lambda_1)\gamma^5 v(p_2, \lambda_2)\phi(z, k_\perp) , \qquad (10) \\ M_0^2 &= \frac{m_{\bar{Q}}^2 + k_\perp^2}{z} + \frac{m_Q^2 + k_\perp^2}{1-z} . \end{aligned}$$

In principle, the momentum distribution amplitude $\phi(z, k_\perp)$ can be obtained by solving the LF QCD bound state equation [33]. However, before such first-principle solutions are available, we would have to be contented with phenomenological amplitudes. One example that has been used is the Gaussian-type wave function [34–36]

$$\phi(z, k_\perp) = N \sqrt{\frac{1}{N_c} \frac{dk_z}{dz}} \exp\left(-\frac{\vec{k}^2}{2\omega_M^2} \right) , \qquad (11)$$

where $N = 4(\pi/\omega_M^2)^{\frac{3}{4}}$, $\vec{k} = (k_\perp, k_z)$, and k_z is defined through

$$z = \frac{E_Q + k_z}{E_Q + E_{\bar{Q}}} , \quad 1 - z = \frac{E_{\bar{Q}} - k_z}{E_Q + E_{\bar{Q}}} , \quad E_i = \sqrt{m_i^2 + \vec{k}^2} \qquad (12)$$

by

$$k_z = \left(z - \frac{1}{2} \right) M_0 + \frac{m_{\bar{Q}}^2 - m_Q^2}{2M_0} , \quad M_0 = E_Q + E_{\bar{Q}} , \qquad (13)$$

and $dk_z/dz = E_Q E_{\bar{Q}}/z(1-z)M_0$. After integrating over p_3^- in Eq. (3), we obtain

$$\begin{aligned} A[Q\bar{Q} \to \gamma^*(q_1)\gamma^*(q_2)] &= e_Q e_{\bar{Q}} N_c \int_0^{q_2^+} dp_3^+ \int \frac{d^2 p_{3\perp}}{2(2\pi)^3 \prod_{i=1}^3 p_i^+} \left[\frac{\Lambda_P}{P^- - p_{1\mathrm{on}}^- - p_{3\mathrm{on}}^-} (I|_{p_3^- = p_{3\mathrm{on}}^-}) \right. \\ &\quad \left. \times \frac{1}{q_2^- - p_{2\mathrm{on}}^- - p_{3\mathrm{on}}^-} + (\epsilon_1 \leftrightarrow \epsilon_2,\, q_1 \leftrightarrow q_2) \right] + (p_{1(3)} \leftrightarrow p_{3(1)}) , \end{aligned} \qquad (14)$$

and

$$\begin{aligned} I &= \mathrm{Tr}[\gamma_5(-\not{p}_3 + m_{\bar{Q}})\, \not{\epsilon}_2(\not{p}_2 + m_Q)\, \not{\epsilon}_1(\not{p}_1 + m_Q)] , \\ p_{i\mathrm{on}}^- &= \frac{m_i^2 + p_{i\perp}^2}{p_i^+} \end{aligned} \qquad (15)$$

where the subscript $\{on\}$ stands for the on-shell particles. One can extract the vertex function Λ_P from Eqs. (3), (10), and (14), given by [32,40,41]

$$\frac{\Lambda_P}{P^- - p_{1\mathrm{on}}^- - p_{3\mathrm{on}}^-} = \frac{\sqrt{p_1^+ p_3^+}}{\sqrt{2[M_0^2 - (m_Q - m_{\bar{Q}})^2]}} \phi(z, k_\perp) . \qquad (16)$$

To calculate the trace I, we use the definitions of the LF momentum variables $[z(x), k_\perp(k_\perp')]$ and take the frame with the transverse momentum $(P - q_2)_\perp = 0$ for the $Q\bar{Q}$ state (P) and photon (q_2) in Fig. 1(a). Hence, the relevant quark variables are

$$\begin{aligned} &p_1^+ = zP^+, p_3^+ = (1-z)P^+, \quad p_{1\perp} = zP_\perp - k_\perp, \\ &p_{3\perp} = (1-z)P_\perp + k_\perp , \\ &p_2^+ = xq_2^+, \quad p_3^+ = (1-x)q_2^+, \quad p_{2\perp} = xq_{2_\perp} - k_\perp', \\ &p_{3\perp} = (1-x)q_{2_\perp} + k_\perp' . \end{aligned} \qquad (17)$$

At the quark loop, it requires that

$$k_\perp = (z - x)q_{2_\perp} + k_\perp' . \qquad (18)$$

$$F_{\pi^0\to\gamma^*\gamma^*}(q_1^2,q_2^2) = -\frac{4}{3}\sqrt{\frac{N_c}{6}}\int \frac{dx\, d^2k_\perp}{2\,(2\pi)^3}\left\{\Phi(z,k_\perp^2)\frac{m_Q+(1-z)m_Q k_\perp^2\Theta}{z(1-z)q_2^2-\left(m_Q^2+k_\perp^2\right)} + (q_2\leftrightarrow q_1)\right\} + (Q\leftrightarrow \bar{Q})\,, \tag{19}$$

with

$$\Phi(z,k_\perp^2) = N\sqrt{\frac{z(1-z)}{2M_0^2}}\sqrt{\frac{dk_z}{dz}}\exp\left(-\frac{\vec{k}^2}{2\omega_M^2}\right),\quad \vec{k}=(\vec{k}_\perp,\vec{k}_z)\,,\quad x=zr\,,\quad \Theta=\frac{1}{\Phi(z,k_\perp^2)}\frac{d\Phi(z,k_\perp^2)}{dk_\perp^2}\,,$$
$$r=\frac{q_2^+}{P^+}=\frac{(m_\pi^2+q_2^2-q_1^2)+\sqrt{\left(m_\pi^2+q_2^2-q_1^2\right)^2-4q_2^2m_\pi^2}}{2m_P^2}\,. \tag{20}$$

Numerical result. To numerically evaluate the transition form factor of $\pi^0\to\gamma^*\gamma$, we need to specify the parameters in Eq. (19). To constrain the quark masses of $m_{u,d,s}$ and the pion scale parameter of ω_π, we use the meson decay constant f_{π^0} and the decay branching ratio of $\pi^0\to 2\gamma$, given by the particle data group (PDG) [42]

$$f_{\pi^0} = 130\,\text{MeV},\ \mathcal{B}(\pi^0\to 2\gamma) = (98.832\pm 0.034)\,\% \tag{21}$$

where the explicit expressions of f_{π^0} [43] and $\mathcal{B}(\pi^0\to 2\gamma)$ are

$$f_{\pi^0} = 4\frac{\sqrt{N_c}}{\sqrt{2}}\int\frac{dx\,d^2k_\perp}{2(2\pi)^3}\,\phi(x,k_\perp)\,\frac{m}{\sqrt{m^2+k_\perp^2}}\,, \tag{22}$$

and

$$\mathcal{B}(\pi^0\to 2\gamma) = \frac{(4\pi\alpha)^2}{64\pi\Gamma_\pi}m_\pi^3|F(0,0)_{\pi^0\to 2\gamma}|^2\,, \tag{23}$$

respectively. As an illustration, we extract $|F(0,0)_{\pi^0\to 2\gamma}| = 0.274$ in GeV^{-1}, $m=m_u=m_d=0.24$, and $\omega_\pi=0.31$ in GeV, which will be used in our following numerical calculations.

We now consider the case with one of the photons on the mass shell. From Eq. (19), the transition pion form factor becomes

$$F_{\pi\gamma}(Q^2)\equiv F_{\pi^0\to\gamma^*\gamma}(Q^2,0)$$
$$=\frac{4\sqrt{2}}{3}\sqrt{\frac{N_c}{3}}\left\{\int\frac{dx\,d^2k_\perp}{2\,(2\pi)^3}\Phi(z,k_\perp^2)\frac{m+(1-z)mk_\perp^2\Theta}{z(1-z)Q^2-(m^2+k_\perp^2)} - \int\frac{dx\,d^2k_\perp}{2\,(2\pi)^3}\Phi(z,k_\perp^2)\frac{m+(1-z)mk_\perp^2\Theta}{(m^2+k_\perp^2)}\right\}. \tag{24}$$

In Fig. 2, we show the form factor in Eq. (24). We note that the first term in Eq. (24) dominates for the lower region of Q^2 and thus it can be use to describe the experimental data of BABAR [1], CLEO [44], and CELLO [45] with

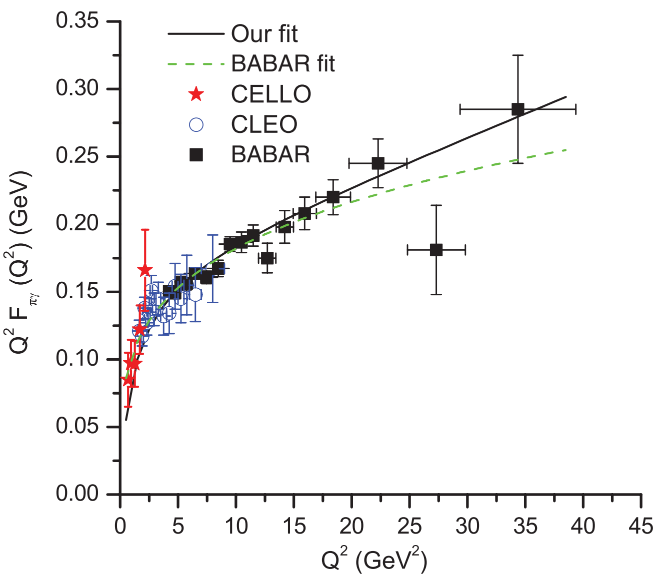

FIG. 2. (Color online) Q^2 dependence of $F_{\pi\gamma}(Q^2)$ in the LFQM. Please set "BaBar" all caps in legend and throughout.

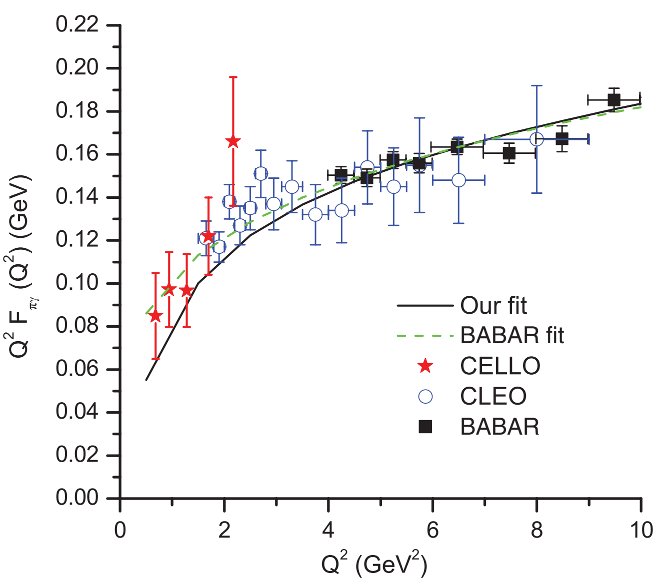

FIG. 3. (Color online) $F_{\pi\gamma}(Q^2)$ for $Q^2 < 10$ GeV^2 in the LFQM.

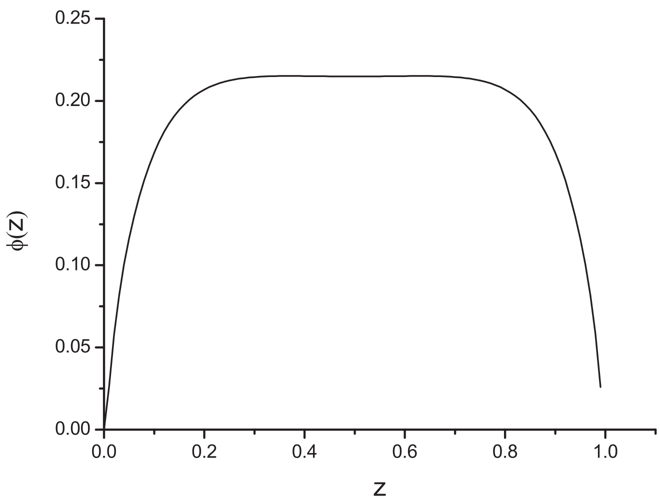

FIG. 4. $\phi(z)$ as a function of z in the LFQM.

$Q^2 \leqslant 10$ GeV^2. The second term in Eq. (24), related to the nonvalence quark contributions, is small for a small Q^2, but it may enhance the form factor with a high value of Q^2. As a result, we will include this term in our numerical calculations. To easily examine the Q^2 dependence of the form factor, we have fitted our result in terms of the double-pole form

$$F_{\pi\gamma}(Q^2) = \frac{F_{\pi\to\gamma\gamma}(0,0)}{M + (\beta Q)^2 - (\alpha Q)^4}\,. \quad (25)$$

Explicitly, we find that the dimension parameters of $\alpha = 0.325, \beta = 1.15$, and $F_{\pi^0\to\gamma\gamma}(0,0) = 0.274$ in GeV^{-1}, and the dimensionless parameter of $M = 3.6$. In Fig. 3, we concentrate on the behavior of the form factor in the region with $Q^2 < 10$ GeV^2. It is easy to see that our results fit the data well in this region similar to other theoretical calculations as expected.

In Fig. 4, we show the DA, $\phi(z)$, as the function of the momentum fraction of the internal quark and meson longitudinal momenta, z, obtained by the integration of $k_\perp$ in Eq. (11).

As we mentioned in the introduction, the BABAR result cannot be fitted by extending the study in Ref. [37] to a high Q^2. The main reason is due to the choices of the free parameters, such as the quark masses and ω_π, leading to a different sharpness of the pion wave function. Similarly, the main difference between our results and those in Ref. [38] comes from DAs. In particular, our DA shown in Fig. 4 appears to be much broader. We note that in Refs. [8–12], a broader DA of the pion is utilized to fit the BABAR data, particularly in the high-Q^2 region. The results in these models differ slightly from ours only at large values of Q^2. It is interesting to point out that our result is almost identical with that in the Regge model [21] and the double logarithmic behavior from the chiral anomaly effects [28]. Finally, we remark that the single data point at $Q^2 = 27.31$ GeV^2 by BABAR, which is apparently consistent with the QCD asymptotic limit, cannot be explained by this work within the framework of the LFQM.

Conclusion. We have studied the form factors of $\pi^0 \to \gamma^*\gamma$ within the LFQM. In our calculation, we have adopted the Gaussian-type wave function and evaluated the form factors for the momentum dependencies in the all allowed Q^2 region. We have also parametrized the form factor in terms of the double-pole form. Our numerical values are close to the experimental results by BABAR. In particular, our results of the transition form factor fit well with the experimental data in the high-Q^2 region, which cannot be explained in the previous attempts based on the framework of the LFQM. Finally, we remark that due to the large uncertainty in the high-Q^2 region for the BABAR data, further theoretical studies as well as more precise experimental data are clearly needed. If some future experiment could not confirm the BABAR data but be rather in agreement with the QCD asymptotic limit, the parameters of the LFQM in this study should be either modified or ruled out.

This work was partially supported by National Center of Theoretical Science and National Science Council (NSC-97-2112-M-471-002-MY3 and NSC-98-2112-M-007-008-MY3) of R.O.C.

[1] B. Aubert *et al.* (The BABAR Collaboration), Phys. Rev. D **80**, 052002 (2009).
[2] G. P. Lepage and S. J. Brodsky, Phys. Rev. D **22**, 2157 (1980).
[3] G. P. Lepage and S. J. Brodsky, Phys. Lett. B **87**, 359 (1979).
[4] V. L. Chernyak and A. R. Zhitnitsky, Nucl. Phys. B **201**, 492 (1982); **214**, 547 (1983).
[5] A. P. Bakulev, S. V. Mikhailov, and N. G. Stefanis, Phys. Lett. B **508**, 279 (2001); **590**, 309(E) (2004).
[6] B. Melic, B. Nizic, and K. Passek, Phys. Rev. D **65**, 053020 (2002); B. Melic, D. Muller, and K. Passek-Kumericki, *ibid.* **68**, 014013 (2003).
[7] S. V. Mikhailov and N. G. Stefanis, Nucl. Phys. B **821**, 291 (2009); Mod. Phys. Lett. A **24**, 2858 (2009).
[8] A. V. Radyushkin, Phys. Rev. D **80**, 094009 (2009).
[9] M. V. Polyakov, JETP Lett. **90**, 228 (2009).
[10] S. Nogeura and V. Vento, Eur. Phys. J. A **46**, 197 (2010).
[11] A. E. Dorokhov, arXiv:1003.4693 [hep-ph]; JETP Lett. **92**, 707 (2010).
[12] X. G. Wu and T. Huang, Phys. Rev. D **82**, 034024 (2010).
[13] A. P. Bakulev, S. V. Mikhailov, and N. G. Stefanis, Phys. Rev. D **67**, 074012 (2003); Phys. Lett. B **578**, 91 (2004).
[14] A. Bzdak and M. Praszalowicz, Phys. Rev. D **80**, 074002 (2009).
[15] H.-n. Li and S. Mishima, Phys. Rev. D **80**, 074024 (2009).
[16] H. L. L. Roberts, C. D. Roberts, A. Bashir, L. X. Gutierrez-Guerrero, and P. C. Tandy, Phys. Rev. C **82**, 065202 (2010).
[17] X. G. Wu and T. Huang, Phys. Rev. D **84**, 074011 (2011).
[18] M. Belicka, S. Dubnicka, A. Z. Dubnickova, and A. Liptaj, Phys. Rev. C **83**, 028201 (2011).
[19] P. Lichard, Phys. Rev. D **83**, 037503 (2011).
[20] S. S. Agaev, V. M. Braun, N. Offen, and F. A. Porkert, Phys. Rev. D **83**, 054020 (2011).
[21] W. Broniowski and E. R. Arriola, arXiv:1008.2317 [hep-ph]; Phys. Rev. D **81**, 094021 (2010).
[22] P. Kroll, arXiv:1012.3542 [hep-ph].
[23] M. Gorchtein, P. Guo, and A. P. Szczepaniak, arXiv:1102.5558 [nucl-th].
[24] S. J. Brodsky, F. G. Cao, and G. F. de Teramond, Phys. Rev. D **84**, 033001 (2011); **84**, 075012 (2011).

[25] A. P. Bakulev, S. V. Mikhailov, A. V. Pimikov, and N. G. Stefanis, Phys. Rev. D **84**, 034014 (2011).
[26] F. Zuo, Y. Jia, and T. Huang, Eur. Phys. J. C **67**, 253 (2010); F. Zuo and T. Huang, arXiv:1105.6008 [hep-ph].
[27] N. G. Stefanis, arXiv:1109.2718 [hep-ph].
[28] T. N. Pham and X. Y. Pham, Int. J. Mod. Phys. A **26**, 4125 (2011).
[29] D. Melikhov, I. Balakireva, and W. Lucha, arXiv:1108.2430 [hep-ph]; W. Lucha and D. Melikhov, arXiv:1110.2080 [hep-ph]; I. Balakireva, W. Lucha, and D. Melikhov, arXiv:1110.5046 [hep-ph]; arXiv:1110.6904 [hep-ph].
[30] A. Stoffers and I. Zahed, Phys. Rev. C **84**, 025202 (2011).
[31] N. G. Stefanis, A. P. Bakulev, S. V. Mikhailov, and A. V. Pimikov, arXiv:1111.7137 [hep-ph].
[32] W. Jaus, Phys. Rev. D **41**, 3394 (1990); **44**, 2851 (1991).
[33] K. G. Wilson, T. S. Walhout, A. Harindranath, W. M. Zhang, R. J. Perry, and S. D. GlazekPhys. Rev. D **49**, 6720 (1994).
[34] C. Q. Geng, C. C. Lih, and W. M. Zhang, Phys. Rev. D **57**, 5697 (1998); **62**, 074017 (2000); Mod. Phys. Lett. A **15**, 2087 (2000).
[35] C. C. Lih, C. Q. Geng, and W. M. Zhang, Phys. Rev. D **59**, 114002 (1999).
[36] C. Q. Geng, C. C. Lih, and C. C. Liu, Phys. Rev. D **62**, 034019 (2000); C. H. Chen, C. Q. Geng, C. C. Lih, and C. C. Liu, *ibid.* **75**, 074010 (2007).
[37] Chien-Wen Hwang, Phys. Rev. D **64**, 034011 (2001).
[38] J. P. B. C. de Melo and T. Frederico, PoSLC **2010**, 063 (2010).
[39] H. J. Melosh, Phys. Rev. D **9**, 1095 (1974).
[40] Demchuk *et al.*, Phys. Atom. Nucl. **59**, 2152 (1996); Int. J. Mod. Phys. A **23**, 3204 (2008).
[41] C. H. Chen, C. Q. Geng, and C. C. Lih, Phys. Rev. D **77**, 014004 (2008); Int. J. Mod. Phys. A **23**, 3204 (2008); Phys. Rev. D **83**, 074001 (2011); C. C. Lih, J. Phys. G **38**, 065001 (2011).
[42] Particle Data Group, Phys. Lett. B **667**, 1 (2008).
[43] H. Y. Cheng, C. Y. Cheung, and C. W. Hwang, Phys. Rev. D **55**, 1559 (1997); C. W. Hwang, *ibid.* **64**, 034011 (2001).
[44] J. Gronberg *et al.* (The CLEO Collaboration), Phys. Rev. D **57**, 33 (1998).
[45] H. J. Behrend *et al.* (The CELLO Collaboration), Z. Phys. C **497**, 401 (1991).